α-Catenin is essential in intestinal adenoma formation

Hiroyuki Shibata*†‡, Hiroshi Takano*§, Masaki Ito*, Hisashi Shioya*, Morihisa Hirota*, Hiroshi Matsumoto*, Yuichi Kakudo†‡, Chikashi Ishioka†‡, Tetsu Akiyama¶, Yumi Kanegae‖, Izumu Saito‖, and Tetsuo Noda*§**††

*Department of Cell Biology, Japanese Foundation for Cancer Research, Cancer Institute, Tokyo 135-8550, Japan; †Department of Clinical Oncology, Institute of Aging, Development, and Cancer, ‡Tohoku University Hospital, and §Center for Translational and Advanced Animal Research on Human Disease, Tohoku University, Sendai 980-8575, Japan; ¶Laboratory of Molecular and Genetic Information, Institute for Molecular and Cellular Biosciences, University of Tokyo, Tokyo 113-0032, Japan; ‖Laboratory of Molecular Genetics, Institute of Medical Science, University of Tokyo, Tokyo 108-8639, Japan; and **Mouse Functional Genomics Research Group, RIKEN Genomic Sciences Center, Kanagawa 244-0804, Japan

Edited by Bert Vogelstein, The Sidney Kimmel Comprehensive Cancer Center at Johns Hopkins, Baltimore, MD, and approved September 27, 2007 (received for review June 19, 2007)

A loss-of-function mutation in the *APC* gene initiates colorectal carcinogenesis. Although the molecular mechanism of tumor initiation is complex, several modifier genes have been identified using mouse models, including the *ApcMin* mouse. Among the familial adenomatous polyposis mouse lines carrying a truncation mutation at codon 580 in *Apc* (*Apc580D*), one line (line19-*Apc*$^{580D/+}$) showed a remarkably reduced incidence of intestinal adenomas (<5% compared with other lines). Extensive genetic analysis identified a deletion in the *α-catenin* (*Ctnna1*) gene as the cause of this suppression. Notably, the suppression only occurred when the *Ctnna1* deletion was in *cis*-configuration with the *Apc580D* mutation. In all adenomas generated in line19-*Apc*$^{580D/+}$, somatic recombination between the *Apc* and *Ctnna1* loci retained the wild-type *Ctnna1* allele. These data strongly indicate that simultaneous inactivation of *α-catenin* and *Apc* during tumor initiation suppresses adenoma formation in line19-*Apc*$^{580D/+}$, suggesting that *α-catenin* plays an essential role in the initiation of intestinal adenomas. Although accumulating evidence obtained from human colon tumors with invasive or metastatic potential has established a tumor-suppressive role for α-catenin in late-stage tumorigenesis, the role of α-catenin in the initiation of intestinal tumorigenesis is not well documented, especially compared with that of β-catenin. A mouse model used in this study focused on the early stage of tumor initiation and clearly indicated an essential role for α-catenin. Thus, α-catenin has dual roles in intestinal tumorigenesis, a supporting role in tumor initiation, and a suppressive role in tumor progression.

APC | modifier

Germline mutations in the adenomatosis polyposis coli (*APC*) gene cause familial adenomatous polyposis (FAP) (1, 2), and somatic mutations in *APC* are frequently found in sporadic colorectal cancers (3, 4). The most well studied functions of APC in colorectal carcinogenesis are its association with multiprotein complexes and its role in β-catenin degradation. APC can bind cytosolic β-catenin together with the scaffold protein, axin, and glucose synthase kinase 3β (5, 6). This kinase phosphorylates the N-terminal serine/threonine residues of β-catenin. Phosphorylated β-catenin is then degraded by ubiquitin-dependent proteosomes (7). In tumor cells with a loss-of-function mutation in *APC*, β-catenin escapes degradation and diffuses into the nucleus where it binds lymphoid enhancer-binding factor-1/T cell-factor family proteins such as TCF4, acts as a transcriptional activator for target genes such as of c-MYC and cyclinD1, and contributes to cell growth (8, 9, 10).

The adherens junction (AJ) complex is composed of a transmembrane protein, E-cadherin, and catenins, including α-, β-, γ-, and p120 (11, 12). The AJ complex is linked to the actin cytoskeleton by α-catenin (13). This linkage maintains barrier function, polarity, migration, and differentiation of epithelial cells (11, 12). Unlike β-catenin, however, the contribution of α-catenin to colorectal carcinogenesis remains unclear. It has been observed that α-catenin expression increases during adenoma formation in the Min mouse (*Apc*$^{Min/+}$) (14).

The significance of α-catenin in adenoma formation may exceed our expectations. Genetic studies indicate that some types of genes modify *APC*-derived adenoma formation. The first example was that the status of the secretory phospholipase A2 gene was responsible for this phenotype (15, 16). To date, several modifier genes, including epidermal growth factor receptor (17), insulin-like growth factor II (18), 5-cytosine DNA methyltransferase (19), and matrilysin (20) have been identified. Identification of a modifier gene that affects *Apc*-derived tumorigenesis will lead to a better understanding of the precise molecular mechanisms of colorectal carcinogenesis.

Results

Establishment of a FAP Mouse Line Exhibiting a Suppressor Phenotype. Heterozygous ES cells carrying the floxed exon 14 of *Apc* (*Apc*$^{580S/+}$) were infected with a Cre expression adenovirus (AxCre) to delete exon 14 and generate *Apc*$^{580D/+}$ (Fig. 1*A*) (21). Of >30 ES subclones isolated after AxCre infection, all carried the *Apc580D* allele, and 10 mutant mouse lines were established. All but one line (line 19) showed the typical intestinal polyposis phenotype. The average number of tumors in F_1 mice from three representative *Apc*$^{580D/+}$ lines (lines 1, 8, and 40) was 125.6 ± 50.3 per mouse (n = 12, ≈14 weeks old) [Fig. 1 *B* and *C* and supporting information (SI) Table 1]. This phenotype was consistently observed after successive backcrossing to C57BL/6J (B6) mice. The average lifespan of the *Apc*$^{580D/+}$ lines was 22.5 ± 4.6 weeks (n = 22), and the main causes of death were intestinal obstruction and hemorrhaging (Fig. 1*D*).

However, the average number of intestinal tumors in line 19 F_1 mice was 6.6 ± 8.6, even at 32 weeks of age (Fig. 1*B* and SI Table 1). This suppressed phenotype was consistent in all F_1, N_2, and N_3 mice at this point, when we had obtained ≈50 mice in total by backcrossing (Fig. 1*C*). In line 19, the average lifespan of heterozygotes was prolonged to 69.0 ± 20.6 weeks (n = 16), reflecting the low tumor incidence (Fig. 1 *C* and *D*).

To identify the molecular basis of this suppressed phenotype, we first confirmed that the *Apc580S* to *Apc580D* alteration had occurred in line19-*Apc*$^{580D/+}$. Southern blotting and sequencing

Author contributions: H. Shibata and T.N. designed research; H. Shibata, H.T., M.I., H. Shioya, M.H., H.M., and Y. Kakudo performed research; T.A., Y. Kanegae, and I.S. contributed new reagents/analytic tools; H. Shibata, C.I., and T.N. analyzed data; and H. Shibata and T.N. wrote the paper.

The authors declare no conflict of interest.

This article is a PNAS Direct Submission.

††To whom correspondence should be addressed. E-mail: tnoda@jfcr.or.jp.

This article contains supporting information online at www.pnas.org/cgi/content/full/0705730104/DC1.

MEDICAL SCIENCES

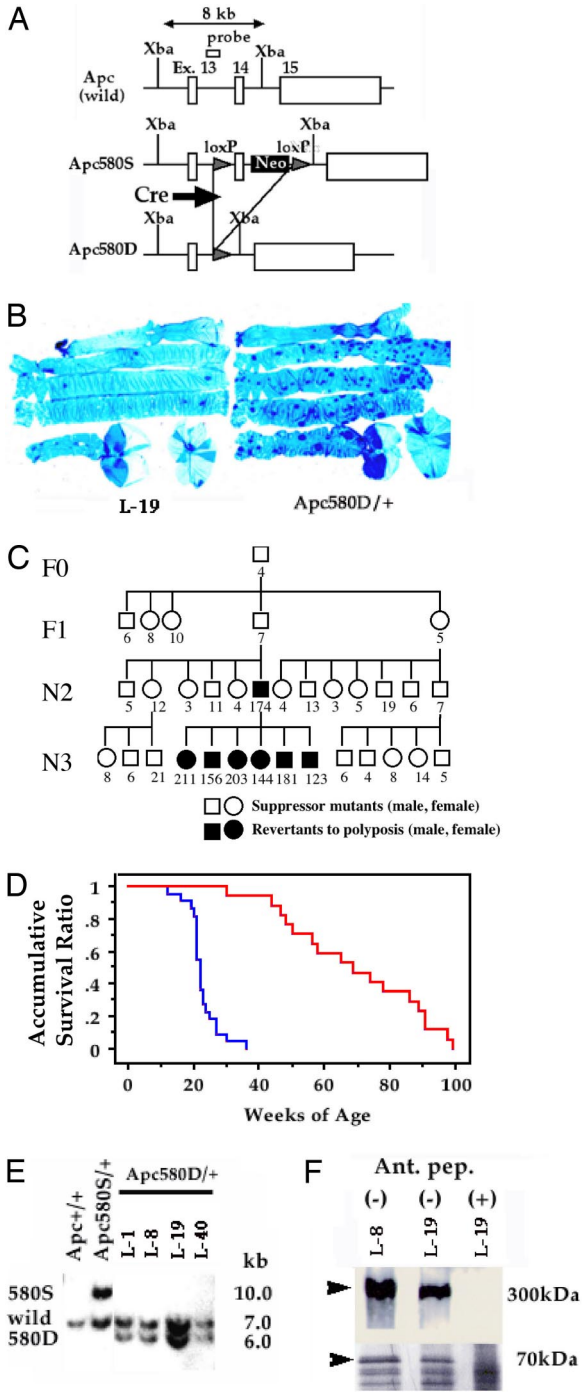

Fig. 1. Analysis of the suppressor mutant, line19-*Apc*$^{580D/+}$. (*A*) Schematic of the deletion in exon 14 after Cre expression. The filled rectangle (Neo) indicates the pGK-*Neo* cassette. (*B*) Phenotype of line19-*Apc*$^{580D/+}$. The total gastrointestinal tract from stomach to rectum was stained with methylene blue dye. Representative samples from line19-*Apc*$^{580D/+}$ (L-19, 50 weeks of age) (*Left*) and from the other *Apc*$^{580D/+}$lines (line8, 14 weeks of age) (*Right*) show the lower tumor incidence in line19-*Apc*$^{580D/+}$. (*C*) Inheritance of the suppressor phenotype in line19-*Apc*$^{580D/+}$ in each generation (F_1, N_2, N_3). Line19-*Apc*$^{580D/+}$ was started from one chimeric mouse (F_0). A representative pedigree of F_1, N_2, and N_3, including revertants, is shown. Numbers indicate the incidence of intestinal tumors. Squares indicate males, circles indicate females, filled symbols indicate revertants, and open symbols indicate suppressors. (*D*) Kaplan–Meier analysis of accumulative survival rate of line19-*Apc*$^{580D/+}$. The red and blue lines indicate line19-*Apc*$^{580D/+}$ and the other *Apc*$^{580D/+}$ line, respectively ($P < 0.001$). (*E*) Southern blot analysis of the *Apc* locus. The probe detected a 7.0-kb fragment in the wild-type allele, a 10.0-kb fragment in the *Apc580S* allele, and a 6.0-kb fragment in the *Apc580D* allele after digestion with XbaI (3). The genetic alteration of the *Apc* allele in line19-*Apc*$^{580D/+}$ (L-19) is identical to that in the other *Apc*$^{580D/+}$ lines, including lines 1, 8, and 40 (L-1, -8, and -40, respectively). (*F*) Western blot analysis of the *Apc* gene product derived from the *Apc580D* allele. A polyclonal antibody recognizing the N-terminal region of APC detected a truncated product (70 kDa) from the *Apc580D* allele as well as the full-length product (300 kDa) in brain lysates from *Apc*$^{580D/+}$ mice. Bands below 70 kDa are nonspecific reactions because they were unchanged in the presence of antigenic peptide (Ant. pep).

analysis of the deletion boundary showed the correct genomic alteration in all *Apc*$^{580D/+}$ lines, including line 19 (Fig. 1*E*). RT-PCR and subsequent sequencing analysis of mRNA obtained from the intestines of *Apc*$^{580D/+}$ mice also confirmed the precise deletion of exon 14 in all *Apc*$^{580D/+}$ lines. *Apc* mRNA expression levels in line 19 were identical to those in the other *Apc*$^{580D/+}$ lines (data not shown). Western blot analysis detected a mutant *Apc* product derived from *Apc580D* with the expected size and comparable expression in all *Apc*$^{580D/+}$ lines, including line 19 (Fig. 1*F*). Further backcrossing of line19-*Apc*$^{580D/+}$ was performed and phenotypic analysis showed that two of 224 mice had severe anemia and large numbers (220 and 174) of intestinal tumors. In addition, this phenotype was observed in all *Apc*$^{580D/+}$ offspring ($n = 8$) derived from these two revertants. Through these analyses, we concluded that the *Apc580D* allele of line 19 was identical to that of the other lines but an additional mutation conferring the suppressed phenotype had been introduced into the ES genome of line 19 in close proximity to the *Apc* locus. From the phenotypic linkage and segregation in line19-*Apc*$^{580D/+}$, we estimated the genetic distance between *Apc* and this "suppressor" locus to be ≈1 centimorgan (reversion frequency 2/224 = 0.89%).

Mapping of the Candidate Locus for the Suppressor Phenotype. To finely map this locus, we used polymorphisms between B6 and 129/Sv. The suppressor mutation should have been introduced in the genome of an ES subclone, which was derived from a J1 ES cell with a 129/Sv origin. Analysis of polymorphic markers on ch.18 suggested that the candidate locus was located in a region distal to *Apc* (Fig. 2). However, analysis of two revertants (N_2 and N_3) suggested that the locus was located in a region distal to D18Mit232, because one of two revertants retained heterozygosity at D18Mit232 (Fig. 2). Next, polymorphic analyses of more than three revertants showed that the candidate locus was located in the region proximal to Rp23/16882, because 73H9TP2Frp, a neighboring marker of Rp23/16882 located in a proximal region, was consistently heterozygous in all of these mutants (Fig. 2). The candidate locus was restricted to the region between D18Mit232 (232) and Rp23/168815rp (Rp23). According to the physical map provided by the Sanger Institute, these markers are located 0.7 and 3.5 MB from the *Apc* locus respectively. As a result, we successfully localized the candidate locus within a ≈2.8-Mb region restricted by two polymorphic markers, D18Mit232 and Rp23/16882 (Fig. 2), and the physical distance between the *Apc* gene and this region is consistent with the genetic distance obtained from the backcrossed mice.

Identification of a Deletion Mutation in the *Ctnna1* Locus. According to the data from the Sanger Institute, at least 79 predicted transcription units, including 55 protocadherin superfamily genes, *Lrrtm2*, *Sil1-pending*, *Paip2*, *Matrin3*, *Ctnna1*, *Ube2d3*, *Cxxc5*, *Slc4a9*, *4BP3*, *Apbb3*, *Slc35a4*, *Dnd1*, *Harsl*, *Slc25a2*, *Slc23a1*, *Pura*, *Ndufa2*, *Ik*, *Hars*, *Cd14*, *Taf7*, and *Nrg2*, are located in this interval (Fig. 2). Mutation screening was conducted for all of these genes by RT-PCR on cDNA obtained from the intestine, liver, and brain of line19-*Apc*$^{580D/+}$. The sizes and sequences of the cDNA fragments were analyzed and

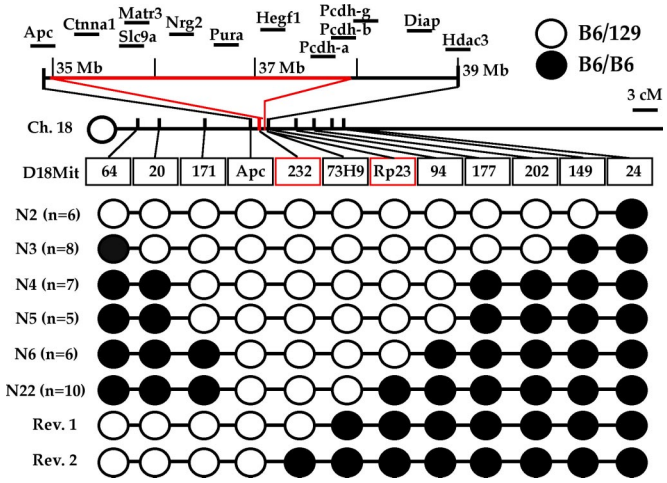

Fig. 2. Mapping of the candidate locus responsible for the suppressed phenotype. A representative genotyping of suppressor mutants and revertants (Rev) for each generation are shown. The candidate locus is indicated by the red line. The open circles denote heterozygosity for 129/Sv (129) and B6, and the filled circles denote homozygosity for B6. The genetic markers are abbreviated: for example, ''64'' is D18Mit64, and ''73H9'' is 73H9TP2Frp. N*x* indicates the number of backcrossing. Candidate genes are represented by symbols (4).

compared with those obtained from the other $Apc^{580D/+}$ lines. The expression levels of all genes were also analyzed by comparing the density of fragments amplified by RT-PCR. No significant changes were detected for any of these genes except *Ctnna1*. RT-PCR analysis of the *Ctnna1* cDNA N-terminal fragment detected a fragment in line19-$Apc^{580D/+}$ that was smaller (790 bp) and weaker than the normal fragment (1,080 bp) (Fig. 3*A*). The band intensity of the unexpected fragment was less than one-third of the normal fragments. Sequence analysis of this shorter fragment showed a deletion in a region corresponding to exons 3 and 4 of *Ctnna1* (Fig. 3*A*) that resulted in a frame-shift mutation at codon 101.

The expression levels of mutant *Ctnna1* transcripts were reduced, perhaps by nonsense-mediated decay of the mutant mRNA. Southern blot analysis showed rearrangement of the *Ctnna1* locus in line19-$Apc^{580D/+}$ (Fig. 3*B*) with an apparent ≈4-kb genomic fragment deleted from the *Ctnna1* locus. Long-range PCR analysis of the genomic DNA around the deletion showed that a shorter fragment of 0.75 kb was additionally amplified together with a 5.0-kb fragment from the wild-type allele in line 19 (Fig. 3*B*). Sequence analysis indicated a 4107-bp deletion encompassing exons 3 and 4 (Fig. 3*B*). In addition to the reduced expression levels caused by nonsense-mediated decay, we assumed that the mutant α-catenin product, which was truncated at codon 101, lost the ability to associate with β-catenin, γ-catenin, and actin (12, 22). Therefore, we concluded that this deletion in the *Ctnna1* locus (*Cat-del* mutation) generated a null allele. Genotyping analysis showed that all suppressor mutants of line19-$Apc^{580D/+}$ carried the *Cat-del* mutation but that it was always absent in the revertants of line19-$Apc^{580D/+}$ as well as in the other $Apc^{580D/+}$ lines (Fig. 3*C*). We speculated that the *Cat-del* mutation was responsible for the suppressed phenotype of line19-$Apc^{580D/+}$.

Expression of α-Catenin in Adenomas from line19-$Apc^{580D/+}$. Adenoma formation is initiated by inactivation of the wild-type *APC* allele and loss of heterozygosity (LOH) of *Apc* is observed in almost all adenoma cases. In addition, gene conversion is considered a major cause of this LOH (23). In the present study, loss of the wild-type *Apc* allele derived from the B6 strain was

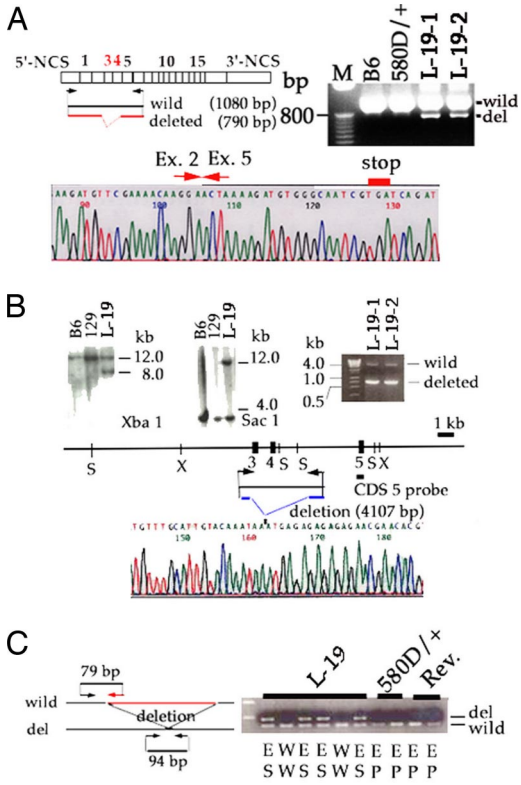

Fig. 3. Identification of a deletion mutation in the *Ctnna1* locus. (*A*) Unusual transcript from the *Ctnna1* gene in line19-$Apc^{580D/+}$. (*Upper Left*) The complementary DNA structure is shown. The boxes indicate the exons, and the arrows represent the RT-PCR primers. (*B*) Identification of the deletion breakpoint in the *Ctnna1* locus. Southern blot analysis was conducted on DNA derived from line19-$Apc^{580D/+}$ (L-19), B6, and 129/Sv (129). The restriction map indicates the sites for SacI (S) and XbaI (X) around exon 5 of *Ctnna1*. An unexpected 8-kb fragment (for a 12-kb wild-type allele) was detected after XbaI digest, and an unexpected 12-kb fragment (for a 4-kb wild-type allele) was detected after SacI digest. Long-range PCR was performed with the primers (arrows) noted on the map. (*C*) (*Right*) Correlation between the suppressed phenotype and the *Cat-del* mutation in line 19. (*Left*) PCR primers (arrows) for genotyping the wild-type allele and the deleted allele of *Ctnna1* (del) are depicted. Genotype of the *Apc* allele and the phenotype of each mutant are denoted at the bottom (E, $Apc^{580D/+}$; W, $Apc^{+/+}$; P, polyposis; S, suppressed phenotype; and W, wild type).

observed in all adenomas of the $Apc^{580D/+}$ lines, including line 19 (Fig. 4*A*). In almost all adenomas (85.8%) of the Apc^{580D} lines except line 19, loss of the wild-type *Ctnna1* allele derived from the B6 strain was also observed.

In contrast, in all line 19 adenomas, although LOH was also observed for the *Ctnna1* locus, the 129/Sv allele was also lost, causing retention of the wild-type *Ctnna1* allele derived from B6 (Fig. 4 *A* and *B*). This result strongly suggested that α-catenin depletion was prevented by retention of the wild-type *Ctnna1* allele. Immunohistochemical analyses (Fig. 4*C*) and Western blotting (Fig. 4*D*) confirmed α-catenin expression in line 19 adenomas. LOH analysis was also performed for the loci flanking *Apc* and *Ctnna1*, and its pattern strongly suggested that somatic recombination might have occurred between the *Apc* and *Ctnna1* loci in the adenomas of line 19, possibly before the *Apc* LOH. This somatic recombination changed the configuration of *Apc580D* and the *Cat-del* mutations from *cis* to *trans* and resulted in retention of wild-type *Ctnna1*. The narrow interval between the *Apc* and *Ctnna1* loci where somatic recombination should occur to retain wild-type *Ctnna1* reflects the suppressed phenotype in line 19.

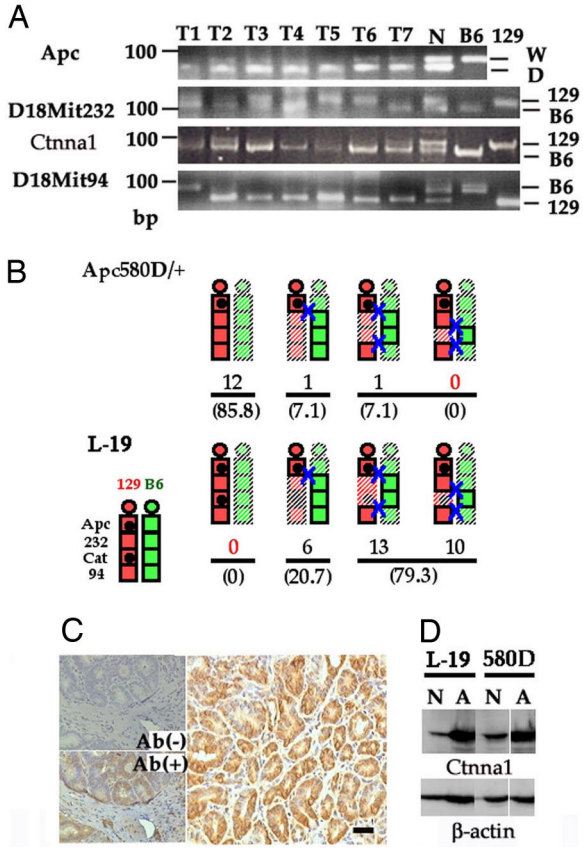

Fig. 4. α-Catenin status in adenomas of line19-*Apc*$^{580D/+}$. (*A*) LOH analysis of the adenomas in line19-*Apc*$^{580D/+}$. Representative LOH analyses of *Apc*, D18Mit232, *Ctnna1*, and D18Mit94 loci in tumor DNA (T1 to T7) are shown. DNA obtained from the normal epithelia of hybrid F_1 mouse of line19 (N), B6, and 129/SV were used as markers. (*B*) Schematic representation of LOH patterns observed in the adenomas of *Apc*$^{580D/+}$ lines. The *Apc* and *Ctnna1* loci on Ch. 18 are depicted. Each allele derived from 129/SV or B6 is colored in red or green, respectively. (*Inset*) Each box corresponds to the designated locus. The dot indicates *Apc580D* or *Cat-del* mutation. The shaded boxes indicate allelic losses, and blue crosses denote somatic recombination. The frequency (top number) and percentage (shown in parenthesis) of each LOH pattern are shown. (*C*) (*Lower Left*) Immunohistochemical analysis of α-catenin in an adenoma from line19-*Apc*$^{580D/+}$. (*Right*) All adenoma cells were highly reactive for α-catenin. (Scale bar, 3 μm.) (*Upper Left*) The specificity of the reaction was confirmed in the absence of antibody [Ab(−)]. (*D*) Western blot analysis of α-catenin of line19-*Apc*$^{580D/+}$. Normal enterocytes were collected from tumor-free ileum by slight scraping of the mucosa with the edge of a glass slide to minimize stromal cell contamination. α-Catenin was overexpressed in the adenoma (A) of line19-*Apc*$^{580D/+}$, as well as the other *Apc*$^{580D/+}$ lines, compared with their normal epithelia (N). α-Catenin expression in the normal epithelium of line19-*Apc*$^{580D/+}$ was reduced by 50% compared with the other *Apc*$^{580D/+}$ line.

Additional somatic recombinations occurred frequently (79.3%) in the region distal to the *Ctnna1* locus in line 19 and in other *Apc*$^{580D/+}$ lines (14.2%) (Fig. 4*B*). This finding suggested that somatic recombination might occur between homologous regions more frequently than expected.

In normal enterocytes of line 19, full-length α-catenin was expressed at levels less than half of that in the other *Apc*$^{580D/+}$ lines (Fig. 4*D*). However, like *Apc*$^{Min/+}$, α-catenin expression was up-regulated in line 19 adenomas to the same level as in the other *Apc*$^{580D/+}$ lines (Fig. 4*D*) (14). Our results indicate that simultaneous ablation of Apc and α-catenin blocks adenoma formation.

Effect of Heterozygous *Ctnna1* Mutations on Adenoma Formation in *Apc*$^{580D/+}$. During backcrossing to B6, we obtained simple *Cat-del* mutation herterozygotes (*Apc*$^{+/+}$, *Ctnna1*$^{\text{Cat-del}/+}$) in line19-*Apc*$^{580D/+}$ (SI Fig. 5*A*). Among 267 offspring, two simple *Cat-del* heterozygotes (*Apc*$^{+/+}$, *Ctnna1*$^{\text{Cat-del}/+}$) were obtained from 120 *cis*-compound heterozygotes (*Apc*$^{580D/+}$, *Ctnna1*$^{\text{Cat-del}/+}$). This frequency (2/122 = 1.64%) closely resembled the reversion frequency (0.89%) of line19-*Apc*$^{580D/+}$. To examine the effect of heterozygous Cat-del mutations on adenoma formation, we crossed the two types of simple heterozygotes, *Cat-del* (*Apc*$^{+/+}$, *Ctnna1*$^{\text{Cat-del}/+}$) and *Apc580D* (*Apc*$^{580D/+}$, *Ctnna1*$^{+/+}$). In the resultant *trans*-compound heterozygotes (*Apc*$^{+/580D}$, *Ctnna1*$^{\text{Cat-del}/+}$), the average number of intestinal tumors was 132.25 ± 68.08, whereas it was 128.58 ± 50.28 for the simple *Apc580D* heterozygotes (*Apc*$^{580D/+}$, *Ctnna1*$^{+/+}$). There was no significant difference in the incidence of intestinal tumor formation or tumor distribution between the two groups (SI Fig. 5*B*). The *trans*-compound heterozygotes and the simple *Apc580D* heterozygotes showed similar phenotypes that were typical of polyposis, including anemia, tarry stool, and body weight loss at ≈15 weeks of age and with an average lifespan of 19.19 ± 0.22 weeks (SI Fig. 5*C*). This indicates that the heterozygous *Cat-del* mutation itself does not affect the tumorigenicity of the *Apc580* mutation; rather the simultaneous ablation of α-catenin with Apc prevents intestinal adenoma formation.

Discussion

In this study, we showed that a deletion mutation in the α-catenin gene, which is located ≈1.0 MB from the *Apc* gene, is responsible for the suppressed phenotype of line19-*Apc*$^{580D/+}$. Adenoma formation in *Apc* mutant mice is initiated by the loss of wild-type *Apc*. In most *Apc* mutant mouse lines, loss of the wild-type *Apc* allele is caused by somatic recombination and results in LOH of the *Apc* allele (23). In this study, all adenomas generated in *Apc580D* mutants including line19 had LOH of the *Apc* allele. A previous report showed that the frequency of somatic recombination is strongly influenced by the degree of polymorphisms among homologous chromosomes (24) and raised the possibility that an α-catenin deletion mutant might reduce the incidence of adenoma formation by suppressing mitotic recombination. This hypothesis, however, was not supported by the results that an α-catenin mutation did not suppress adenoma formation when it was located in *trans*-configuration to *Apc*. However, the fact that all adenomas in line19-*Apc*$^{580D/+}$, including very small adenomas, retained the wild-type α-catenin allele as a result of somatic recombination between two loci strongly suggests that functional α-catenin is indispensable for adenoma cell growth and/or survival during or right after the loss of the *Apc* gene in the early stages of polyp formation.

In epithelial cells, α-catenin resides in an AJ complex consisting of E-cadherin, β-catenin, and other molecules where it links the AJ complex to the actin cytoskeleton (11, 12). Under physiological conditions, AJs are lost during the detachment of enterocytes, which subsequently undergo apoptosis (anoikis) (22). In *Drosophila* larval epithelia loss of DE-Cadherin, which also resides in AJs and plays an equivalent role to E-cadherin in mammalian epithelial tissues, causes cells to sort out from wild-type cells (2, 25). These results suggest that the loss of AJs in intestinal epithelial cells might cause apoptosis or exclude cells from surrounding epithelial tissues. Furthermore, α-catenin overexpression can suppress the canonical pathway of Wnt signaling mediated by β-catenin (26, 27), and activation of Wnt signaling induced by the loss of Apc causes apoptotic cell death in some mouse tissues (28). These results also raise the possibility that over activated Wnt signaling might affect the survival of α-catenin-deficient adenoma cells. However, there is accumulating evidence suggesting that α-catenin and/or functional AJs are not essential for epithelial cell survival. For example, in mouse mammary gland epithelium, simultaneous ablation of E-cadherin and p53 induces primary tumors without the AJ complex (29). Conditional ablation of *Ctnna1* in the skin leads

to keratinocyte hyperproliferation that resembles squamous cell carcinoma (30). Furthermore, cell lines can be established from *Ctnna1* knockout embryos despite the lethality of *Ctnna1* knockout mice (31). Therefore, the detailed function of α-catenin in the early stages of adenoma formation remains to be elucidated.

The indispensableness of α-catenin in the early stages of adenoma formation in *Apc* mutant mice fits well with the observation that α-catenin expression is increased in intestinal adenomas in humans as well as *Apc* mutant mice. In contrast, reports of reduced α-catenin expression in colorectal cancer specimens with invasive or metastatic potential and deletions of the α-catenin gene from human colorectal cancer cells have established a tumor suppressive role for α-catenin in the late stage of colorectal tumorigenesis (32, 33). Therefore, our study interestingly proposes dual roles for α-catenin in colorectal carcinogenesis, a supporting role in the early stage and a suppressive role in the late stage. In sequences from human colorectal adenoma-carcinomas, activating Ras mutations are frequently detected in large-sized adenomas but not in small ones (34). Interestingly, several studies have reported a relationship between Ras activation and reduced AJ function, including α-catenin expression (30, 35, 36). Therefore, Ras activation might correspond to the transition of two alternative roles for α-catenin in colorectal tumorigenesis. The precise mechanism of synergic interactions between the functional loss of *APC* and the overexpression of α-catenin and between Ras activation and α-catenin reduction remain to be elucidated.

Materials and Methods

Establishment of line19-*Apc*$^{580S/+}$. *Apc*$^{580S/+}$ ES cells were infected with AxCre at a multiplicity of infection (moi) of 15 or 1.5 for 30 min at 37°C. A small proportion of the infected cells (≈10^3 cells) were plated in a 60-mm dish coated with feeder cells. Growing colonies were selected under stereoscopic observation and then isolated. After confirmation of the planned Cre/*loxP* recombination in each ES clone, germ-line chimera were established as described previously. All animal studies were conducted in accordance with guidelines set by the Cancer Institute and Tohoku University.

Mouse Genome Analysis. Mouse genome information was obtained from the Sanger Institute, National Center for Biotechnology Information (www.ensembl.org/Mus_musculus/index.html). STS markers, including the markers described below, were selected among candidate repetitive sequence regions. Polymorphisms in these markers between B6 and 129/Sv were confirmed by sequencing. STS markers and the numbers of polymorphic repetitive sequence markers are shown as B6/129Sv. The amplifying primers were as follows: 73H9TP2Frp marker (CA)21/(CA)15: 73H9TP2Frp(+), 5′-CATGGCAGG; CACTTTACCCACTGA-3′, and 73H9TP2Frp(−), 5′-AGAGCTTAGAGGTCTTTCCTAGGT-3′; Rp23/168815Rp marker (CA)19(TA)15/(CA)21(TA)20: Rp23/168815Rp(+), 5′-GTAAAAACACATGCAAGCATGTAC-3′, and Rp23/168815Rp(−), 5′-AAGAGGGTCAACTATAGATACATG-3′; and Ctnna1–4 marker (GGAA)19/(GGAA)21: Ctnna1–4(+), 5′-CTTAAGAATCAATCAGTTAATCAACCC-3′, and Ctnna1–4(−), 5′-CGGGCTATCCAGTGAAACCCTATC-3′. A restriction map of the *Ctnna1* locus was obtained from the mouse genome. Long-range PCR to identify the *Cat-del* mutation was performed with the following primers: Ctnna1(d)fl(+), 5′-CACATCAGAAGAGCGCATCAGATC-3′; and Ctnna1(d)fl(−), 5′-CACAGTCTCCATCAAAGGCTGTTG-3′.

RNA and cDNA Analysis. Total RNA was extracted from mouse brain, liver, and normal intestine by using TRIzol Reagent (Gibco/BRL, Carlsbad, CA). Five micrograms of total RNA was reverse transcribed using random hexamers to obtain cDNA (First cDNA synthesis kit; Amersham, Piscataway, NJ). RT-PCR for each candidate gene was conducted; for example, the first one-fourth portion of *Ctnna1* cDNA was amplified with the following primers: Ctnna1RT1(+), 5′-CGCCAGTTCGCTGCAGAAATGAC-3′; and Ctnna1RT1(−), 5′-ATTCTGAGAGCAGGTCCTGTAGAG-3′. Sequence analyses were conducted using a Big DyeTM Termination Cycle Sequencing Ready Reaction (Applied Biosystems, Foster City, CA).

Western Blotting and Immunohistochemistry. Western blotting was conducted for Apc as described in ref. 21. α-Catenin was detected using a rabbit anti-α-catenin antibody (×4,000 dilution, C2081; Sigma, St. Louis, MO) and horseradish peroxidase-conjugated mouse anti-rabbit IgG (×2,000 dilution, sc-2357; Santa Cruz Biotechnology, Santa Cruz, CA). Anti-actin antibody (×100 dilution, A2066; Sigma) was used as the internal control.

For immunohistochemistry, deparaffinized 4-μm specimens in 0.01 M citrate buffer were microwaved (500 W) for 15 min. After blocking with normal goat serum and pretreating with 0.3% hydrogen peroxide with added methanol, specimens were treated with C2081 (×2,000 dilution) at 4°C overnight. After treating with biotin-labeled anti-rabbit IgG antibody [Histofine Simple Stain Max-PO(R); Nichirei, Tokyo, Japan], peroxidase-conjugated streptoavidin was added. Finally, 3,3′-diaminobenzidine tetrahydrochloride staining and hematoxylin nuclear staining were conducted.

PCR Genotyping. The *Apc580D* mutation was genotyped with PCR primers Flox(+), 5′-AGGTGGTCATTAGTTTAATCCTGTG-3′; and Flox(−), 5′-ACAGTCAATATAATGCTAGAACTAG-3′.

The *Cat-del* mutation was genotyped with PCR primers cl. 19 del(+), 5′-ATAGCCCGGGATAGCCTGGAATGC-3′; and cl. 19 del(−), 5′-GTTCTGCCTTCCCTCTTTAAAGTC-3′. The paired wild-type allele was amplified by cl. 19 del(−) and cl. 19 wild(+) primers 5′-TTACATTACCAGTACTCTTAGTAG-3′.

LOH Analysis. A 4-μm-thick paraffin-embedded specimen was deparaffinized with xylene and stained with hematoxylin. Using a microscope, 40–80 tumor cells were scraped with a 27-gauge fine needle and treated with 10 μl of lysis buffer [20 mM Tris·HCL (pH 8.0), 1 mM EDTA, 0.5% Tween 20, and 200 μg/ml proteinase K] at 42°C for 5 h. One microliter of sample solution was used for PCR. LOH analyses of the *Apc* locus were conducted using primers Flox(+) and Flox MCS(−), 5′-CTAGTGGATCCGATAACTCCGTATAATG-3′, for amplification of the Apc580D allele. Intron 13(−) 2, 5′-CAGGAACCTTTCATTTACAGTTTC-3′, and Flox(+) primers were used to amplify the normal allele. LOH analyses of the D18Mit232 and D18Mit94 loci were conducted by seminested PCR with the following primers: 232F3(+), 5′-GAAGCTTTTACCTTAGTCACAATG-3′, and 232(−), 5′-CCACGGCTGAATTATTTTGGCTATC-3′; or 94F(+), 5′-TTGGATCCTCAACATATGTC-3′, and 94R(−), 5′-TCATCTGTATAAATGGGTTGACCT-3′ for the first cycle; followed by 232F3(+) and 232R2, 5′-GCTTCCCTAAGTAGCCATTTACTG-3′, or 94F(+) and 94N(−), 5′-GTCTTAACATTCAGATCTTTTAACT-3′. LOH analysis of the *Ctnna1* locus was conducted with the Ctnna1–4(+) and Ctnna1–4(−) primers. Each PCR amplification was followed by a secondary 20-cycle PCR.

Kaplan–Meier Analysis. Kaplan–Meier analysis was performed using Statview 5.0 (SAS Institute, Cary, NC). The log-rank test was used to calculate *P* values.

We thank J. Kuno, H. Yamanaka, and M. Motoki for their technical assistance. This work was supported in part by Core Research for Evolutional Science and Technology of the Japan Science and Technology Corporation.

1. Nishisho I, Nakamura Y, Miyoshi Y, Miki Y, Ando H, Horii A, Koyama K, Utsunomiya J, Baba S, Hedge P (1991) *Science* 253:665–669.
2. Joslyn G, Carlson M, Thliveris A, Albertsen H, Gelbert L, Samowitz W, Groden J, Stevens J, Spirio L, Robertson M, *et al.* (1991) *Cell* 66:601–613.
3. Miyoshi Y, Nagase H, Ando H, Horii A, Ichii S, Nakatsuru S, Aoki T, Miki Y, Mori T, Nakamura Y (1992) *Hum Mol Genet* 1:229–233.
4. Smith KJ, Johnson KA, Bryan TM, Hill DE, Markowitz S, Willson JK, Paraskeva C, Petersen GM, Hamilton SR, Vogelstein B, *et al.* (1993) *Proc Natl Acad Sci USA* 90:2846–2850.
5. Rubinfeld B, Albert I, Porfiri E, Fiol C, Munemitsu S, Polakis P (1996) *Science* 272:1023–1026.
6. Behrens J, Jerchow BA, Wurtele M, Grimm J, Asbrand C, Wirtz R, Kuhl M, Wedlich D, Birchmeier W (1998) *Science* 280:596–599.
7. Orford K, Crockett C, Jensen JP, Weissman AM, Byers SW (1997) *J Biol Chem* 272:24735–24738.
8. Morin PJ, Sparks AB, Korinek V, Barker N, Clevers H, Vogelstein B, Kinzler KW (1997) *Science* 275:1787–1790.
9. He TC, Sparks AB, Rago C, Hermeking H, Zawel L, da Costa LT, Morin PJ, Vogelstein B, Kinzler KW (1998) *Science* 281:1509–1512.
10. Tetsu O, McCormick F (1999) *Nature* 398:422–426.
11. Yap AS, Brieher WM, Gumbiner BM (1997) *Annu Rev Cell Dev Biol* 13:119–146.
12. Kobielak A, Fuchs E (2004) *Nat Rev Mol Cell Biol* 5:614–625.
13. Imamura Y, Itoh M, Maeno Y, Tsukita S, Nagafuchi A (1999) *J Cell Biol* 22:1311–1322.
14. Carothers AM, Melstrom KA, Jr, Mueller JD, Weyant MJ, Bertagnolli MM (2001) *J Biol Chem* 19:39094–39102.
15. MacPhee M, Chepenik KP, Liddell RA, Nelson KK, Siracusa LD, Buchberg AM (1995) *Cell* 81:957–966.
16. Cormier RT, Hong KH, Halberg RB, Hawkins TL, Richardson P, Mulherkar R, Dove WF, Lander ES (1997) *Nat Genet* 17:88–91.
17. Roberts RB, Min L, Washington MK, Olsen SJ, Settle SH, Coffey RJ, Threadgill DW (2002) *Proc Natl Acad Sci USA* 99:1521–1526.
18. Hassan AB, Howell JA (2000) *Cancer Res* 60:1070–1076.
19. Cormier RT, Dove WT (2000) *Cancer Res* 60:3965–3970.
20. Wilson CL, Heppner KJ, Labosky PA, Hogan BLM, Matrisian LM (1997) *Proc Natl Acad Sci USA* 94:1402–1407.
21. Shibata H, Toyama K, Shioya H, Ito M, Hirota M, Hasegawa S, Matsumoto H, Takano H, Akiyama T, Toyoshima K, *et al.* (1997) *Science* 278:120–123.
22. Fouquet S, Lugo-Martinez VH, Faussat AM, Renaud F, Cardot P, Chambaz J, Pincon-Raymond M, Thenet S (2004) *J Biol Chem* 279:43061–43069.
23. Haigis KM, Dove WF (2003) *Nat Genet* 33:33–39.
24. Shao C, Stambrook PJ, Tischfield JA (2001) *Nat Genet* 28:169–172.
25. Le Borgne R, Bellaiche Y, Schweisguth F (2002) *Curr Biol* 12:95–104.
26. Sehgal RN, Gumbiner BM, Reichardt LF (1997) *J Cell Biol* 139:1033–1046.
27. Giannini AL, Vivanco M, Kypta RM (2000) *J Biol Chem* 275:21883–21888.
28. Hasegawa S, Sato T, Akazawa H, Okada H, Maeno A, Ito M, Sugitani Y, Shibata H, Miyazaki Ji J, Katsumi M, *et al.* (2002) *Proc Natl Acad Sci USA* 99:297–302.
29. Derksen PW, Liu X, Saridin F, van der Gulden H, Zevenhoven J, Evers B, van Beijnum JR, Griffioen AW, Vink J, Krimpenfort P, *et al.* (2006) *Cancer Cell* 10:437–449.
30. Vasioukhin V, Bauer C, Degenstein L, Wise B, Fuchs E (2001) *Cell* 104:606–617.
31. Torres M, Stoykova A, Huber O, Chowdhury K, Bonaldo P, Mansouri A, Butz S, Kemler R, Gruss P (1997) *Proc Natl Acad Sci USA* 94:901–906.
32. Vermeulen SJ, Bruyneel EA, Bracke ME, De Bruyne GK, Vennekens KM, Vleminckx KL, Berx GJ, van Roy FM, Mareel MM (1995) *Cancer Res* 55:4722–4728.
33. Raftopoulos I, Davaris P, Karatzas G, Karayannacos P, Kouraklis G (1998) *J Surg Oncol* 68:92–99.
34. Vogelstein B, Fearon ER, Kern SE, Hamilton SR, Preisinger AC, Nakamura Y, White R (1989) *Science* 244:207–211.
35. Espada J, Perez-Moreno M, Braga VM, Rodoriguez-Viciana P, Cano A (1999) *J Cell Biol* 146:967–980.
36. Nam JS, Ino Y, Sakamoto M, Hirohashi S (2002) *Jpn J Cancer Res* 93:1020–1028.